

2nd CIRP Conference on Surface Integrity (CSI)

Surface integrity characteristics of *NiTi* shape memory alloys resulting from dry and cryogenic machining

Y. Kaynak^{a*}, H.E. Karaca^b, I.S. Jawahir^{b,c}

^aMechanics and Machine Elements Division, Marmara University, Goztepe Campus, Kadikoy, 34722, Istanbul, Turkey

^bDepartment of Mechanical Engineering, University of Kentucky, Lexington, KY 40506, USA

^cInstitute for Sustainable Manufacturing (ISM), University of Kentucky, Lexington, KY 40506, USA

* Corresponding author. Tel.: +90 216 3365770; fax: +90 216 3378987. E-mail address: yusuf_kaynak@yahoo.com.

Abstract

NiTi alloys are extensively used in many industries due to their unique properties such as super elasticity, shape memory and phase transformation. Since the *NiTi* alloys have temperature-dependent mechanical and material properties, this work focuses on the effects of dry and cryogenic machining processes on surface integrity characteristics of *NiTi* alloys. Surface quality and topography, microstructure, transformation response and phase transformation temperatures of machined specimens are measured to assess the machining-induced surface integrity characteristics of *NiTi* alloys. Obtained results illustrate that machining of *NiTi* alloys under different cutting and cooling conditions affects their resulting surface integrity characteristics. Moreover, as compared to dry machining, cryogenic machining helps to improve surface quality and has substantial effects on the phase transformation behavior of machined specimens.

© 2014 The Authors. Published by Elsevier B.V. This is an open access article under the CC BY-NC-ND license (<http://creativecommons.org/licenses/by-nc-nd/3.0/>).

Selection and peer-review under responsibility of The International Scientific Committee of the “2nd Conference on Surface Integrity” in the person of the Conference Chair Prof Dragos Axinte dragos.axinte@nottingham.ac.uk

Keywords: Cryogenic machining; surface integrity; *NiTi* shape memory alloys; phase transformation

1. Introduction

The application of shape memory alloys (SMAs) spans a wide variety of industrial sectors such as aerospace, automotive, biomedical, oil exploration [1], seismic isolation, and composite structures for controlling the vibration [2]. New biomaterials are being constantly developed to respond to the need for better mechanical properties and biocompatibility [3]. Since *NiTi* SMAs combine the shape memory effect, super elasticity and other excellent mechanical properties [3], they have great potential for biomedical [4, 5] and aerospace applications [6, 7]. However, due to high work hardening, ductility, superelasticity, shape memory aspects, low modulus of elasticity, highly temperature-dependent behavior of these alloys, rapid and aggressive tool-wear, poor chip breakability, high cutting forces were observed and these leads to increasing manufacturing cost and limits their application in

different industries [8, 9]. Recently, the authors of the current study proposed cryogenic machining as an alternative approach to improve machining performance of *NiTi* alloys. Cryogenic machining is found to be substantially improve the machining performance of these alloys by reducing the progressive tool-wear, force components, and surface roughness as compared to other machining conditions such as preheated, dry [10] and MQL machining [8]. Since *NiTi* shape memory alloys are temperature-sensitive and difficult-to-machine materials, the resulting effects of machining on the material's thermo-mechanical response, especially due to high strain, strain-rate, is much more complex in comparison with other engineering materials [10]. Therefore, an investigation on the machining-induced surface integrity characteristics is required to determine the effects of machining processes to establish process-microstructure-property relation. Jawahir et al. [11] reported that surface integrity characteristics of *Ni* based and *Ti* based alloys have been extensively studied in

detail including various surface quality, microstructure, residual stress, grain refinement and microhardness [12]. However, very limited studies focus on *NiTi* based alloys with machining-induced hardness variation on surface [13], grain refinement and phase transformation, [14], and surface quality of *NiTi* alloys [15, 16].

The major aim of this current study is to contribute to the understanding of the effects of machining process on the resulting surface integrity and shape memory aspects, particularly phase transformation temperature and transformation response, of *NiTi* alloys.

2. Experimental Procedure

The material used in this study was a commercially available, $Ni_{49.9}Ti_{50.1}$ (at %) alloy. The material was received as round bars of 10 mm diameter, in the hot-rolled/hot-drawn and hot-straightened conditions. Cutting length in all machining experiments was 26 mm. Phase transformation temperature of all machined samples was measured via Perkin Elmer Pyris 1 Differential Scanning Calorimetry (DSC). The weight of the samples for DSC measurements varied between 10 to 40 mg, and the heating and cooling rates were kept constant at $10^{\circ}C/min$. The specimens were placed in an aluminum pan. The temperature and energy flow were calibrated using the reference standard. The phase transformation temperatures were determined from DSC peaks using slope line extension method. During measurements, the samples were first heated to $150^{\circ}C$ and held at that temperature one minute, and then cooled to $25^{\circ}C$ at a constant cooling rate. The martensite start, martensite finish, austenite start and austenite finish temperatures were determined from Figure 1 to be 73, 49, 86 and $109^{\circ}C$, respectively. Thus, the *NiTi* alloy was found to be in martensitic phase at room temperature.

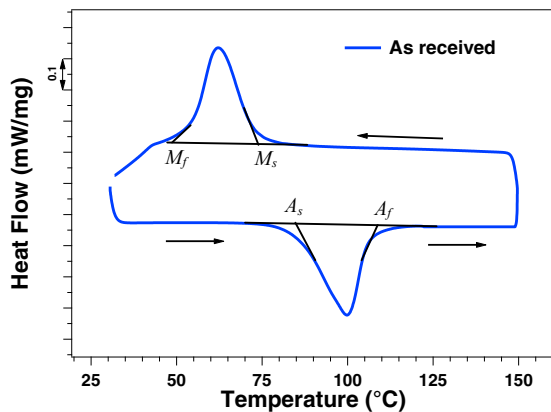


Fig. 1. DSC response of *NiTi* SMAs

Microstructure of as-received material is shown in Figure 2. The alloy is single phase, with a dynamically

recrystallized and equiaxed grain structure with approximately 20-30 μm average grain size [17]. It has to be noted that grain size of as received material was not different in perpendicular plane.

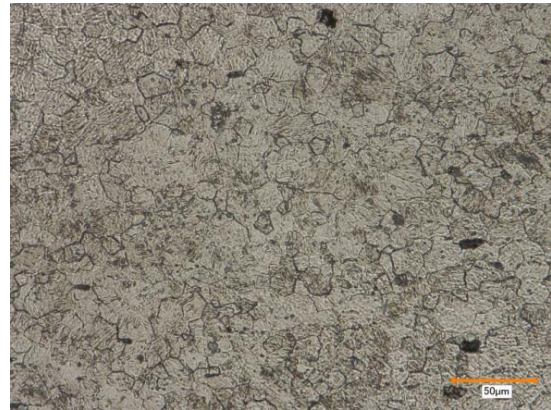


Fig. 2. Microstructure of as-received *NiTi* SMAs

A DCGT 11T308HP cutting tool insert, KC5410 grade with *TiB2* coating, was used in the experiments. According to the tool manufacturer [18], KC5410 insert has a PVD *TiB2* coating over a deformation-resistant unalloyed substrate. The *TiB2* coating is harder than *TiN* and *TiAlN* coatings and has an extremely smooth surface. This results in reduced surface friction, faster chip flow, and outstanding wear resistance. The substrate is unalloyed and fine-grained, and offers sharp edges, and excellent thermal deformation resistance [19]. Edge radius of the tool inserts used in the experiments was very consistent and varied between 18 to 20 μm .

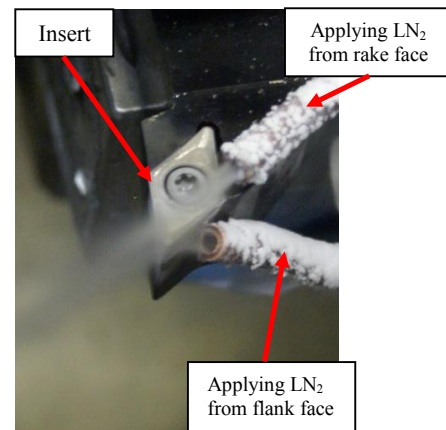


Fig. 3. Cryogenic machining application

The tool holder was SDJCL 12 3B H5M. Machining experiments were conducted on a Mazak CNC turning center. In machining tests, constant feed rate, $f = 0.05$ mm/rev, and depth of cut, $a_p = 0.5$ mm, were used. Selected cutting speeds were 12.5 and 100 m/min. The

cryogenic coolant was liquid nitrogen, applied under 1.5 MPa pressure, and approximately 10 g/s mass flow rate. Application of the cryogenic cooling during the turning operation is shown in Figure 3. Liquid nitrogen was delivered to the cutting region through 4.78 mm diameters two nozzles. One was placed over the rake face of cutting tool, while other was placed at the back of the tool holder to deliver liquid nitrogen towards to cutting tool tip from the rake face of the cutting tool [8].

3. Results

3.1. Surface quality and topography

Figure 4 shows the surface topography of samples machined under dry and cryogenic cooling conditions at the cutting speed of 12.5 m/min. Feed marks on the surface of dry and cryogenically machined samples are visible. There is no big difference on the topography of the dry and cryogenically machined samples except dry machined sample has slightly wider valley of perforated feed marks. However, surface topography of dry and cryogenically machined samples are noticeably different at high cutting speed ($V_c = 100$ m/min) as shown in Figure 5.

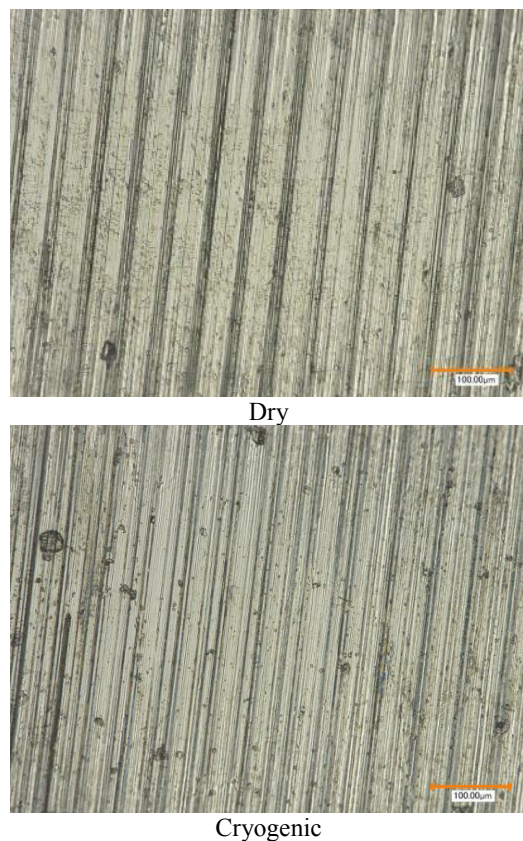


Fig. 4. Surface topography of machined NiTi alloys ($V_c = 12.5$ m/min)

While feed marks are visible on the surface of dry machined sample, much smoother surface was obtained with cryogenic machining. The smoother surface in cryogenic machining at high cutting speed can be attributed to reduced tool-wear and reduced thermal distortion. Cryogenic machining results in decreased surface roughness due to the smoother surface and reduced peaks and valleys on the machined surface, and hence, improved the surface quality, as shown in Fig. 6.

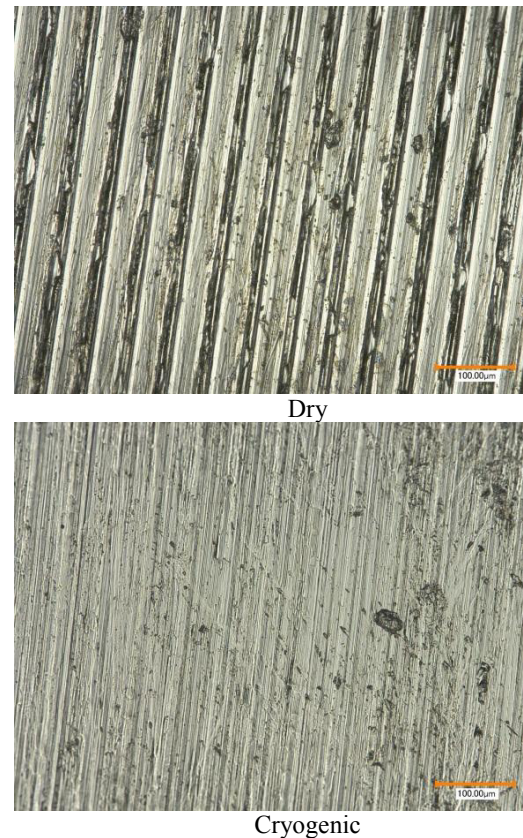


Fig. 5. Surface topography of machined NiTi alloys ($V_c = 100$ m/min)

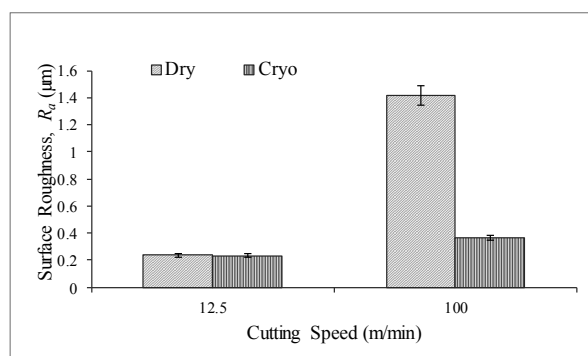


Fig. 6. Surface roughness as a function of cutting speed under dry and cryogenic machining

The surface roughness of cryogenically machined

sample was approximately 0.4 μm and dry machined sample was approximately 1.4 μm . It is a well-known fact that failure or crack generally starts on the surface or subsurface where these deep feed marks could result in stress concentration at the surface and initiate the fracture and failure. Considering the relationship between surface quality and performance of machined products, particularly its contribution to the risk of failure of functional products, in general, a smoother and high quality surface is desired from machining processes. Cryogenic machining meets this demand better than the dry machining.

1.2. Microstructure

Surface and subsurface microstructure of dry and cryogenically machined *NiTi* alloys are shown in Figure 7. Grain refinement was not clearly observed from these optical microscopy images.

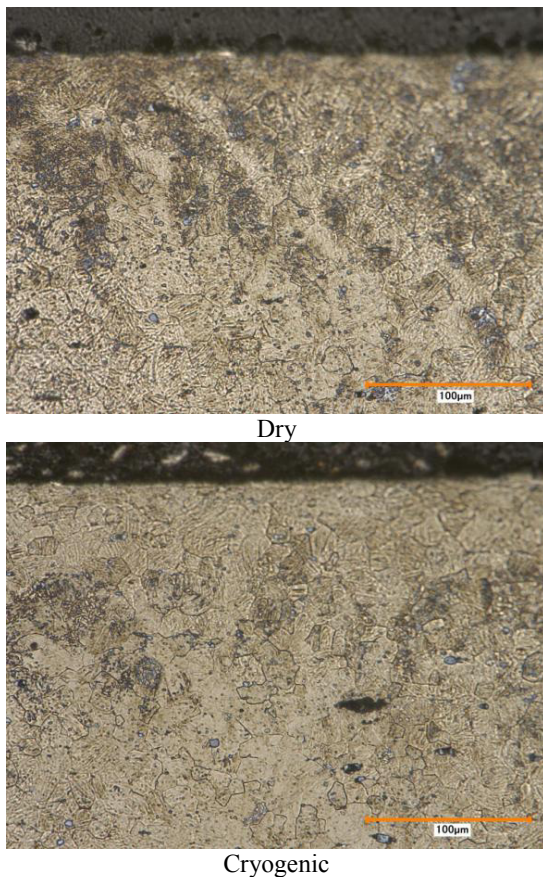


Fig. 7. Surface and subsurface microstructure of machined *NiTi* alloys under dry and cryogenic machining at 100 m/min.

Both samples were etched homogeneously by immersing samples into etchant. It is clear that the reactions of first 125 μm from the top of the samples to etching are

different than the bulk of the material. In other words, grain boundaries in that region are not as visible as grain boundaries in the bulk of the material. Although other analysis such as DSC and X-Ray diffraction (XRD) of these layers confirms the occurring of high dislocation density in this layer, further investigation utilizing transmission electron microscopy (TEM) and scanning electron microscopy (SEM) are required to determine the depth of affected layer and grain refinement on the surface and subsurface of machined *NiTi* samples. It has to be noted that the obtained images from the samples machined at low cutting speed under dry and cryogenic cooling conditions did not show considerable difference.

1.3. Phase transformation temperature and deformation response of machining-induced layer

Our previous studies in machining of room-temperature austenitic *NiTi* alloys revealed that machining process alters the phase transformation temperatures of the surface and subsurface of machined specimens [14]. A DSC measurement of machined surface and subsurface is a reliable and repeatable approach to quantitatively and qualitatively identify the machining-induced phase transformation temperatures of *NiTi* alloy. It also helps to understand whether the examined specimen was subject to any stresses, defects or dislocation density coming from processing by comparing it with as received specimen. Figure 8 shows the DSC response of cryogenically machined sample.

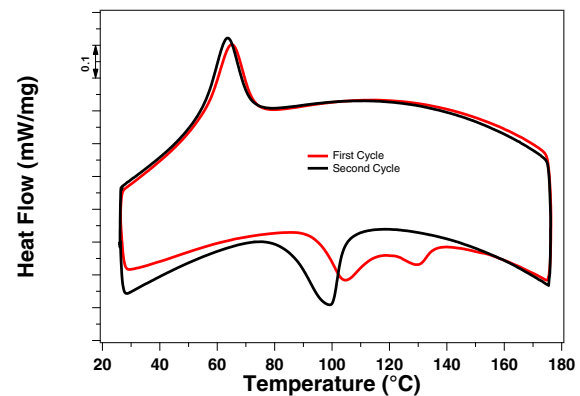


Fig. 8. DSC response of cryogenically machined specimen ($V_c = 100$ m/min)

It is evident that the austenite finish temperature of the surface and subsurface of cryogenically machined sample increased from 109 $^{\circ}\text{C}$ to 140 $^{\circ}\text{C}$ during the first heating cycle. In addition to austenite finish temperature, austenite start temperature of the specimen is also increased and reached to 90 $^{\circ}\text{C}$. The increase in transformation temperatures can be attributed to formation of the residual stress and high dislocation

density and relaxation of elastic energy after machining which suppress and delay the martensite to austenite phase transformation. After first thermal cycle, peak broadening gets smaller and hence both temperatures (A_s and A_f) were reduced and reach close to the as-received temperature. During the first cycle, heating the specimen to 175 °C helped to annihilate the machining effects and consequently, reduced transformation temperatures. Figure 9 shows the DSC response of dry machined sample. Austenite finish temperature slightly increased to approximately 115 °C at the first cycle during heating and a slightly broadened transformation peak during heating was observed.

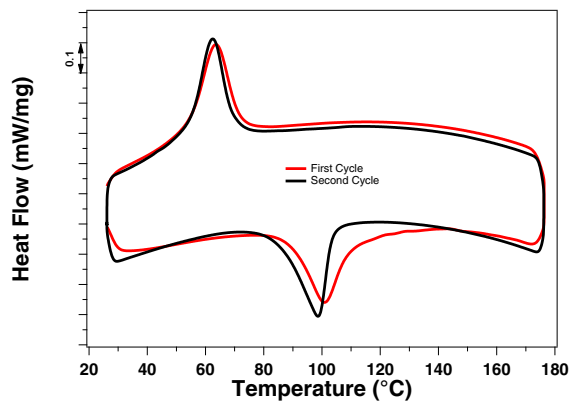


Fig. 9. DSC response of dry machined specimen ($V_c = 100$ m/min)

The comparison of as received, dry machined, and cryogenically machined samples during the first cycle are shown in Figure 10. The largest peak broadening, associated with increased temperature requirement to transform from martensite to austenite phase state, due to martensite stabilization or introduced high dislocation density and consequently reduced amount of transformed material, was observed with cryogenically machined sample.

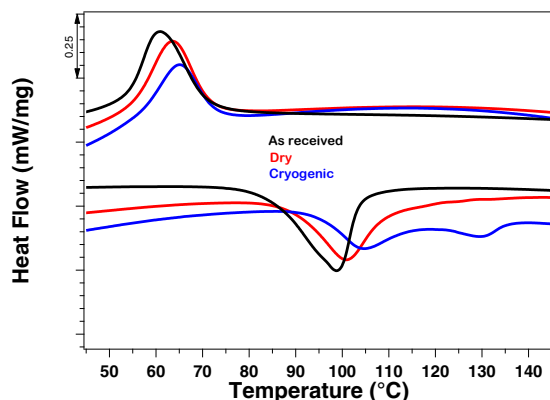


Fig. 10. The comparison of the DSC responses of as received, dry machined and cryogenically machined specimens

These results indicate that residual stress and dislocation density on the surface and subsurface of dry machined samples was much smaller than that of cryogenically machined sample. This study provides evidence that machined surface and subsurface have different phase transformation responses than the as received material.

4. Conclusions

In this study, cryogenic and dry machining-induced surface integrity parameters (surface quality, topography, surface roughness, microstructure and phase transformation temperature) were investigated in machining of *NiTi* alloy. Cryogenic machining process helped to improve the surface quality of machined components more than the dry machining. Although no clear machining-induced layer was observed on both dry and cryogenically machined specimens from the optical microscopy, further examination is required to determine the exact depth of affected layer. Martensite to austenite transformation temperatures are higher and transformation peak is broader in cryogenically machined sample than the dry machined sample which indicates that the cryogenic machining has more severe effects on the surface integrity characteristics of *NiTi* alloys by introducing high dislocation density and residual stresses on their surfaces and subsurface.

Acknowledgements

Authors gratefully acknowledge the support from the NASA FAP Aeronautical Sciences Project and the NASA EPSCOR Program under Grant No NNX11AQ31A. Dr. Yusuf Kaynak also acknowledges the support from Scientific Research Project Program of Marmara University under grant No FEN-D-090414-0109.

References

- [1] Lagoudas, D.C., 2008. Shape Memory Alloys: Modeling and Engineering Applications. New York, Springer.
- [2] Han, Y.L., Li, Q.S., Li, A.Q., Leung, Y.T., Lin, P.H., 2003. Structural vibration control by shape memory alloy damper, *Earthquake Eng Struc* 32, p. 483-94.
- [3] Fadlallah, S.A., El-Bagoury, N., Gad El-Rab, S.M., Ahmed, R.A., El-Ousamii, G., 2014. An overview of *NiTi* shape memory alloy: Corrosion resistance and antibacterial inhibition for dental application, *Journal of Alloys and Compounds* 583, p. 455-64.
- [4] Rondelli, G., 1996. Corrosion resistance tests on *NiTi* shape memory alloy, *Biomaterials* 17, p. 2003-8.
- [5] Shabalovskaya, S.A., 1996. On the nature of the biocompatibility and on medical applications of *NiTi* shape memory and superelastic alloys, *Bio-medical materials and engineering* 6, p. 267-89.
- [6] Hartl, D.J., Lagoudas, D.C., 2007. Aerospace applications of shape memory alloys, *Proc Inst Mech Eng Part G-J Aersp Eng* 221, p. 535-52.
- [7] Calkins, F.T., Mabe, J.H., 2010. Shape Memory Alloy Based

- Morphing Aerostructures, *J Mech Design*, p.1 32.
- [8] Kaynak, Y., Karaca, H.E., Noebe, R.D., Jawahir, I.S., 2013. Tool-wear analysis in cryogenic machining of NiTi shape memory alloys: A comparison of tool-wear performance with dry and MQL machining. *Wear* 306, p. 51-63.
- [9] Weinert, K., Petzoldt, V., 2004. Machining of NiTi based shape memory alloys. *Materials Science and Engineering A* 378, p. 180-4.
- [10] Kaynak, Y., Karaca, H.E., Noebe, R.D., Jawahir, I.S., 2013. Analysis of Tool-wear and Cutting Force Components in Dry, Preheated, and Cryogenic Machining of NiTi Shape Memory Alloys. *Procedia CIRP* 8, p. 498-503.
- [11] Jawahir, I.S., Brinksmeier, E., M'Saoubi, R., Aspinwall, D.K., Quteiro, J.C., Meyer, D., Umbrello, D., Jayal, A.D., 2011. Surface integrity in material removal processes: Recent advances, *Cirp Annals-Manufacturing Technology* 60, p. 603-26.
- [12] M'Saoubi, R., Outeiro, J., Chandrasekaran, H., Dillon, O.W., Jawahir, I.S., 2008. A review of surface integrity in machining and its impact on functional performance and life of machined products. *International Journal of Sustainable Manufacturing* 1, p. 203-36.
- [13] Kaynak, Y., Karaca, H., Jawahir, I.S., 2010. Sustainability evaluation in machining of NiTi shape memory alloy, 1st international Conference on Sustainable Life in Manufacturing (SLIM 2010) p. 40-7.
- [14] Kaynak, Y., Tobe, H., Noebe, R.D., Karaca, H.E., Jawahir, I.S., 2014. The effects of machining on microstructure and transformation behavior of NiTi alloy. *Scripta Materialia* 74, p. 60-63.
- [15] Kaynak, Y., Karaca, H.E., Jawahir, I.S., 2011. Cryogenic machining of NiTi shape memory alloy, 6th Int Conference and Exhibition on Design and Production of Machines and Dies/Molds p. 123-28.
- [16] Guo, Y., Klink, A., Fu, C., Snyder, J., 2013. Machinability and surface integrity of Nitinol shape memory alloy. *CIRP Annals-Manufacturing Technology* 62, p. 83-86.
- [17] Stebner, A., Sisneros, T., Vogel, S., Clausen, B., Brown, D.W., Garg, A., et al. 2013. Micromechanical Elastic, Twinning, and Slip Train partitioning of Polycrystalline Monoclinic Nickel-Titanium Large Uniaxial Deformations Measured via In Situ Neutron Diffraction. *Journal of the Mechanics and Physics of Solids*, accepted for publication.
- [18] www.kennametal.com.
- [19] Zhou, J., Bushlya, V., Avdovic, P., Ståhl, J.E., 2012. Study of surface quality in high speed turning of Inconel 718 with uncoated and coated CBN tools. *The International Journal of Advanced Manufacturing Technology* 58, p. 141-51.